

Position control of shape memory alloy actuators with internal electrical resistance feedback using neural networks

N Ma¹, G Song^{1,3} and H-J Lee²

¹ Department of Mechanical Engineering, University of Houston, Houston, TX 77204, USA

² NASA Glenn Research Center, Cleveland, OH 44135, USA

E-mail: gsong@uh.edu

Received 5 March 2003, in final form 2 February 2004

Published 1 June 2004

Online at stacks.iop.org/SMS/13/777

doi:10.1088/0964-1726/13/4/015

Abstract

The development of a position control system for a shape memory alloy (SMA) wire actuator using an electrical resistance feedback is presented in this paper. A novel control scheme is implemented to eliminate the need for a position sensor to achieve stable and accurate positioning by utilizing the actuator's electrical resistance feedback. Experiments are conducted to investigate the relationship between electrical resistance and displacement using an SMA wire test set-up. Due to the highly nonlinear behavior of the SMA actuator, a neural network is employed to model the relationship and to predict the position of the actuator using only the electrical resistance. Feedback control of the SMA is achieved by using a proportional-derivative (PD) controller. Experimental results demonstrate that the proposed position control system achieves good control performance without using a position sensor.

1. Introduction

In recent years, shape memory alloy (SMA) materials have received increasing attention due to the unique ability to return to a predetermined shape when heated. This inherent property arises as a result of the reversible crystalline phase transformation that occurs between the low temperature martensite and high temperature austenite phases. Although the austenite and martensite phases have the same chemical composition and atomic order, the two phases have different crystallographic structures. Austenite has a body centered symmetric structure that exists at high temperature, while martensite has a low symmetric monoclinic structure that stabilizes at relatively low temperature. When an SMA is cooled from a high temperature, the material undergoes a martensitic transformation from the high temperature austenite. Since the bond energy in the martensite is low, this phase can be easily deformed. In martensite, even after removal of the stress, the strain remains. This residual strain can be recovered by heating the material to the austenite phase,

which causes the SMA to return to the original shape. This response is referred to as the shape memory effect.

During the martensite–austenite transformation, the SMA exhibits a large force against external resistances. A 0.02 inch diameter nickel–titanium alloy (NiTi or Nitinol) wire can lift as much as 16 pounds, which is associated with a 5% length recovery. This high strain property of SMAs offers great potential as actuators in a variety of different applications ranging through micro-robot manipulation [1], aircraft wing shape control [2], and micro-system precision control [3]. In all these applications, precise regulation of the actuator is desired, but presents a significant challenge due to the hysteresis associated with the phase transformation of the SMA actuator.

Previous research has focused on the use of two types of control algorithm to achieve position control of the SMA actuator. The first involves incorporating a reverse dynamic model of the SMA actuator into the control system in order to compensate or reduce the hysteresis effect. Representative models of this SMA actuator include a one-dimensional constitutive model relating the stress to the state variables of the strain, temperature, and martensitic fraction developed by

³ Author to whom any correspondence should be addressed.

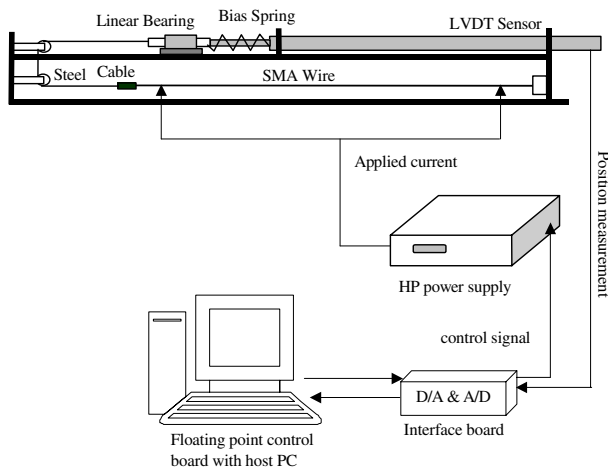


Figure 1. A schematic diagram of the experimental set-up.

Brinson *et al* [4] and a variable sub-layer model of SMAs proposed by Ikuta *et al* [5]. The common drawback in using these models involves an issue of practicality, since many of the required model parameters must be experimentally determined.

The second type of control algorithm relies on a feedback control loop to stabilize the SMA actuator and improve actuation performance. The position, temperature, or electrical resistance (ER) of the SMA actuator is typically used as a state variable in the feedback signal of the control system. Among these state variables, position is the most widely used. The use of a sliding-mode based robust control system using position feedback on an SMA wire actuator was investigated by Song [6]. Through use of a linear variable differential transformer (LVDT) to feed back the SMA location, the capability of a control system with position feedback to accurately control the deflection of the SMA actuator was demonstrated. However, the requirement of a position sensor increases the system cost and size. Feedback control using temperature has also been investigated recently [7]. This research demonstrated that temperature feedback control is not practical due to the difficulty of precisely measuring the disturbed temperature of the SMA actuator in an open environment.

On the other hand, the relationship between the ER variation and strain of an SMA actuator during the transformation is deterministic and repeatable, though highly nonlinear. This behavior arises since, under certain stress conditions, the strain is only a function of the martensite fraction. Since the variation of ER is determined by the martensite fraction (i.e. the transformation degree) and the strain, this behavior allows the use of ER to measure the strain or displacement in order to control an SMA actuator without using a position sensor.

The use of ER feedback in a force control system has been applied to the design of an antagonistic SMA actuator for an active endoscope by Ikuta *et al* [8]. The experimental results demonstrated that the force generated by the antagonistic SMA actuator had a nearly linear relationship with the normalized electrical resistance. However, this observed linear relationship between force and ER generally cannot be extended to spring-biased SMA actuators. In the spring-based

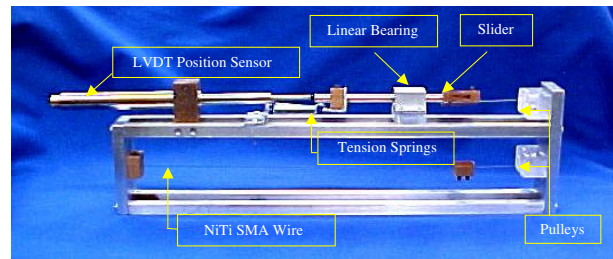


Figure 2. The experimental set-up: the platform.

(This figure is in colour only in the electronic version)

configuration the return force is provided by a bias spring, which in comparison to the antagonistic SMA actuator has a much larger temperature hysteresis. In fact, many other researchers have shown that the ER variation during phase transformations involves a complex interaction of temperature and stress [9–11]. This provides the motivation for the current research to investigate the ER variation for spring-biased SMA actuators.

Recently, an electrical feedback control system for a constantly loaded SMA actuator system was reported by Raparelli *et al* [10]. By using a constant weight to provide the return force, the stress on the SMA actuator remained fixed during the transformation. This resulted in small amount of hysteresis in the relationship between strain and ER that could be neglected, permitting the use of a linear function to approximate the relationship. However, since the ER change is dependent on the stress in the SMA actuator, this research does not provide a general purpose solution to the problem of position control of a spring-biased SMA actuator using electrical resistance feedback.

This paper will present the development a position control system for a spring-biased NiTi wire actuator using electrical resistance feedback. The rest of this paper is organized as follows. Section 2 describes the experimental set-up developed to test the variation of ER and to implement the control system. Section 3 presents experimental results investigating the effect of hysteresis on ER and strain response. Section 4 describes the neural network model employed to approximate the relationship between the displacement and the ER, the proportional-derivative (PD) position control system of the NiTi wire actuator developed, and the result of experimental testing on the control system.

2. Experimental set-up

The experimental set-up is illustrated schematically in figure 1 and contains three major sections: a testing platform, a PC-hosted real-time control system, and a programmable power supply. The testing platform is designed for testing and control of a single NiTi SMA wire as depicted in figure 2. The wire is 228.6 mm in length and 0.381 mm in diameter, and is characterized with a 90 °C austenite-finish temperature. The fixed end of the wire is connected to the platform frame and the moving end is attached to a steel cable. The steel cable is linked to a linear-bearing supported slider through two pulleys that constrains the slider and permits only horizontal movements. The tension spring pulls the SMA wire back to its cold length. Since the goal of this research is position-control of the SMA

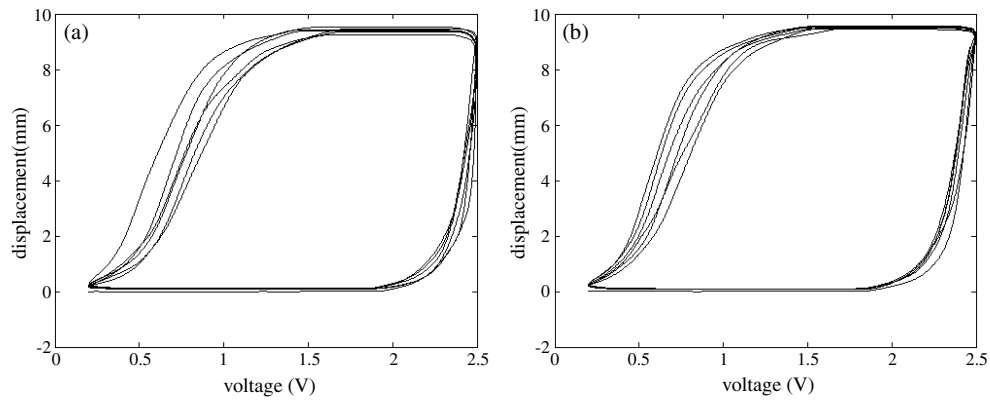


Figure 3. Displacement versus applied voltage in the first test: (a) the first set of data and (b) the second set of data.

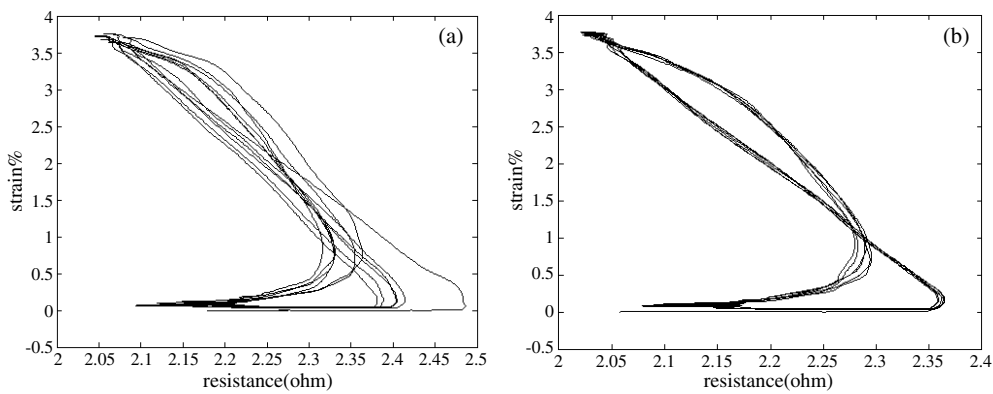


Figure 4. Strain versus ER in the first test: (a) the first set of data and (b) the second set of data.

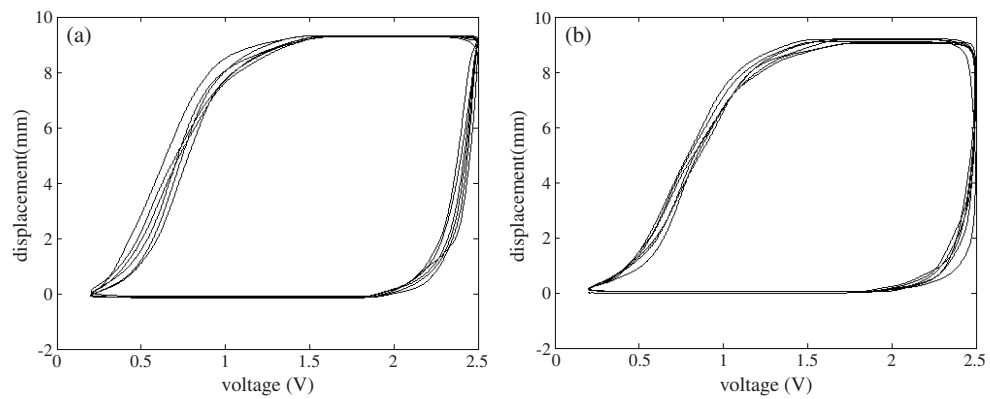


Figure 5. Displacement versus applied voltage in the second test: (a) under small pre-tension and (b) under large pre-tension.

wire actuator, only a position sensor is employed in this set-up and no temperature sensor is used. An LVDT position sensor, whose tip is placed against the slider, is used to measure the displacement of the slider. Pre-tension is applied to the SMA wire through a tension spring. The pre-tension can be adjusted by changing the equilibrium position of the slider at low temperature. In this experimental configuration, the motion of the slider is controlled by the deformation of the SMA wire actuator. When the NiTi wire is electrically heated and undergoes a phase transformation to the stronger austenite, the wire will contract and move the slider. Once the electric current is removed, the wire cools and transforms back to the weaker martensite phase.

3. Testing of the NiTi wire actuator

A series of experiments was conducted to investigate the relationship between ER and displacement of the NiTi wire. These tests were necessary since previous research on ER variation assumed either constant temperature or constant stress conditions. In this research, the SMA wire is subjected to varying stress during the thermally induced transformation that more closely resembles general applications of SMA actuators. In addition, since ER variation is sensitive to many factors, such as heat treatment, composition, and the transformation path, baseline tests for each SMA actuator with ER feedback control must be conducted to provide a reference starting point.

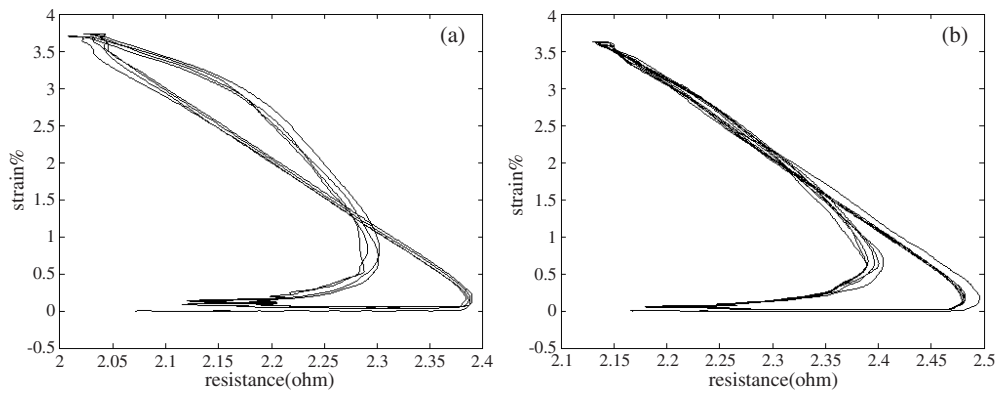


Figure 6. Strain versus ER in the second test: (a) under small pre-tension and (b) under large pre-tension.

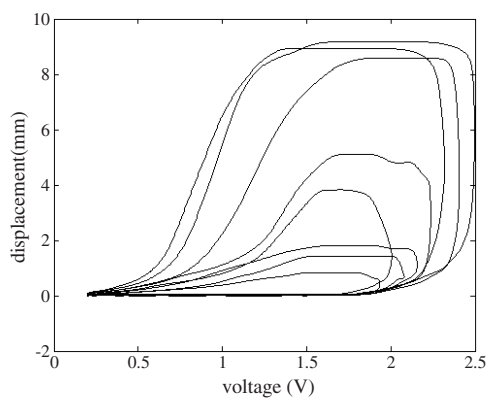


Figure 7. Displacement versus applied voltage.

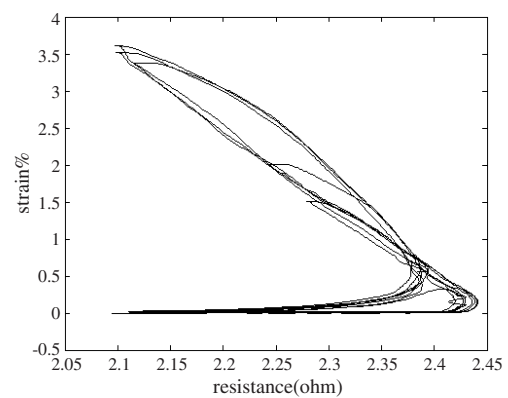


Figure 8. Strain versus ER in the third test.

Open-loop tests were conducted first to explore the relationship between ER and displacement of the spring-biased NiTi wire actuator. A sine-wave voltage signal was used to activate the NiTi wire actuator, using a slow input frequency to ensure full phase transformation of the SMA wire actuator. The tests were conducted under different activation conditions to study the effects of different pre-tensions, different maximum stresses, and different magnitudes of input voltages on ER variation.

In the first set of experiments, the NiTi wire was electrically heated using a 1/60 Hz sine-wave voltage signal with the pre-tension fixed. During the experiment, the ER–displacement curves were observed not to overlap as the experiment progressed. Thus, two sets of the data were collected at different time intervals, which are shown in figures 3 and 4. There are two noticeable phenomena. First, hysteresis is clearly observed in the relationship between ER and strain. In figure 4, the ER values corresponding to the same strain value are different in the heating and cooling processes. Similarly, the slope of the curve varies in each activation cycle. When the wire is heated, but before the transformation takes place, the curve is horizontal (i.e. the slope is zero) and the ER decreases at a nearly constant rate (i.e. the slope is negative) after the wire contracts. In contrast, the ER behaves differently in the cooling process. At the beginning of the martensitic transformation the ER increases at a large rate, and as the transformation advances the increasing rate becomes smaller until the ER decreases (i.e. the slope of the curve continuously

varies from a negative value to a positive value). The ER hysteresis is caused by the difference phase transformations that occur in cooling (i.e. austenite to R-phase to martensite) and heating (i.e. direct martensite to austenite) [9]. Under some conditions in a cooling process, the parent phase (austenite) is transformed to an R-phase, which is then transformed to the martensite phase. Since the R-phase has a crystallographic structure similar to that of the martensite with a large resistance value, the ER value in cooling is larger than that in heating at the beginning of the transformation. In fact, there is a competition between the austenite–martensite transformation and the austenite–R-phase transformation. The decrease of ER at the end of the cooling process is a consequence of the transformation of the R-phase to the martensite.

The second phenomenon observed is that the hysteresis is not stable at the beginning stage of the experiment. Figure 4(a) corresponds to the data recorded in the first 360 s of the test, while figure 4(b) exhibits the ER variation after 900 s of activation (15 activation cycles). The curves only repeat well after being activated for some time. A possible explanation for this phenomenon is that the residual strain gradually decreases to zero after a certain number of activation cycles [11].

A second set of experiments was conducted with different stresses applied on the wire. The maximum stress on the wire can be adjusted by varying the pre-tension on the wire as long as the wire moves the same distance. The results are shown in figures 5 and 6. The larger applied stresses result in a reduced ER hysteresis width. This occurs since, under

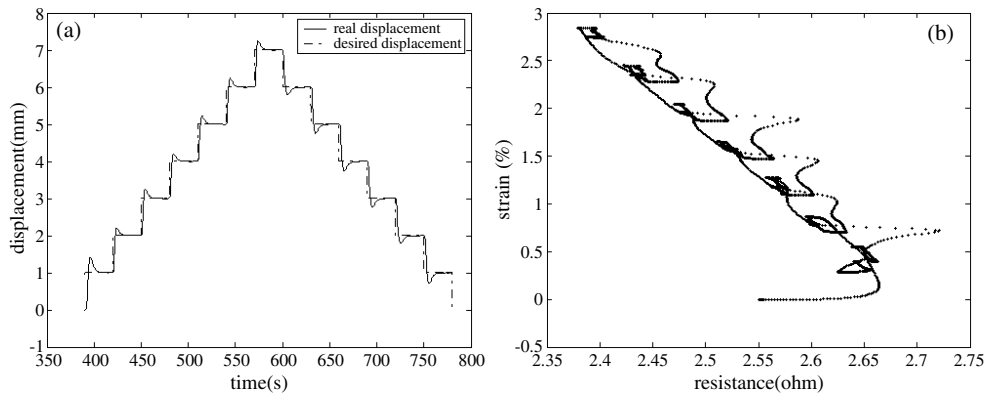


Figure 9. The results of the closed-loop preliminary test: (a) system response and (b) strain versus ER.

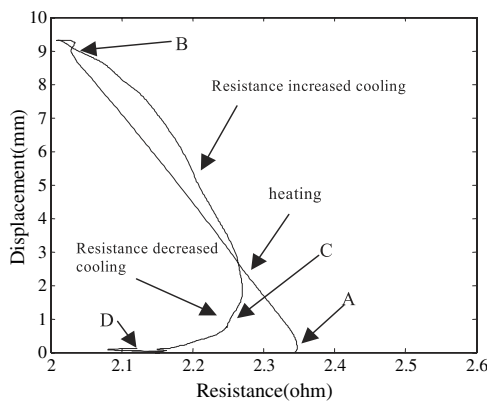


Figure 10. The representative hysteresis loop used for the neural network training.

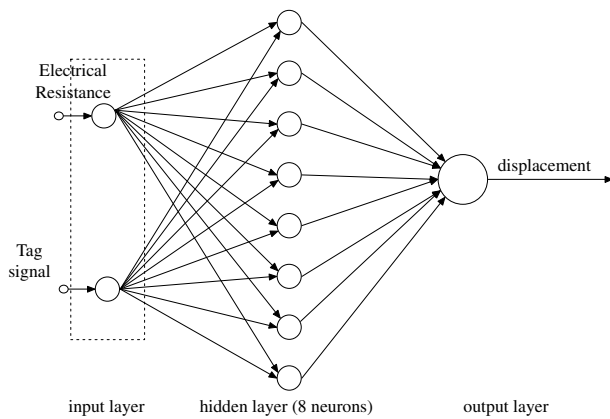


Figure 11. The structure of the neural network.

higher stress conditions, the amount of austenite transformed to R-phase is reduced and more austenite is directly transformed into martensite [11, 12]. In addition, a larger pre-tension decreases the range of ER change while increasing the ER value for the same strain when compared to the case with a small pre-tension.

In contrast to the previous two sets of experiments in which the transformations were fully completed in each cycle, a third set of experiments was conducted to study the ER variation during the uncompleted transformation using a decaying sine-wave voltage signal. The magnitude of the

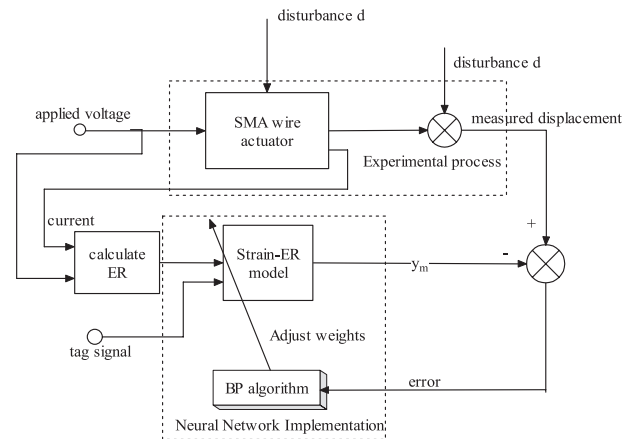


Figure 12. A schematic diagram illustrating the training of the neural network.

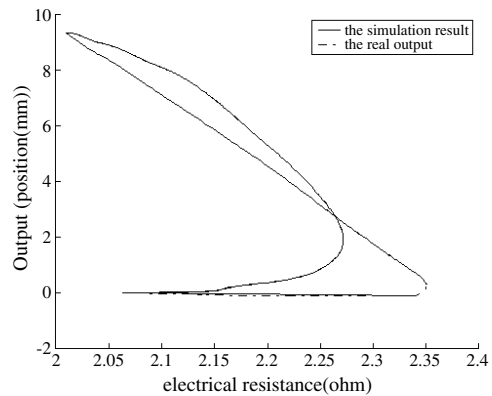


Figure 13. Comparison of the simulation result and the real output.

applied voltage gradually decreased from 2.5 to 1.9 V in 360 s. The experimental results depicted in figures 7 and 8 show that the minor hysteresis loops corresponding to the uncompleted transformations are enclosed by the major loop of the completed transformation. In addition, the minor loops eventually converge to the major loop as the actuating voltage increases.

To further study the ER variation, a closed-loop test was conducted using a PD position controller. A multi-step command was used as input with the PD controller ensuring

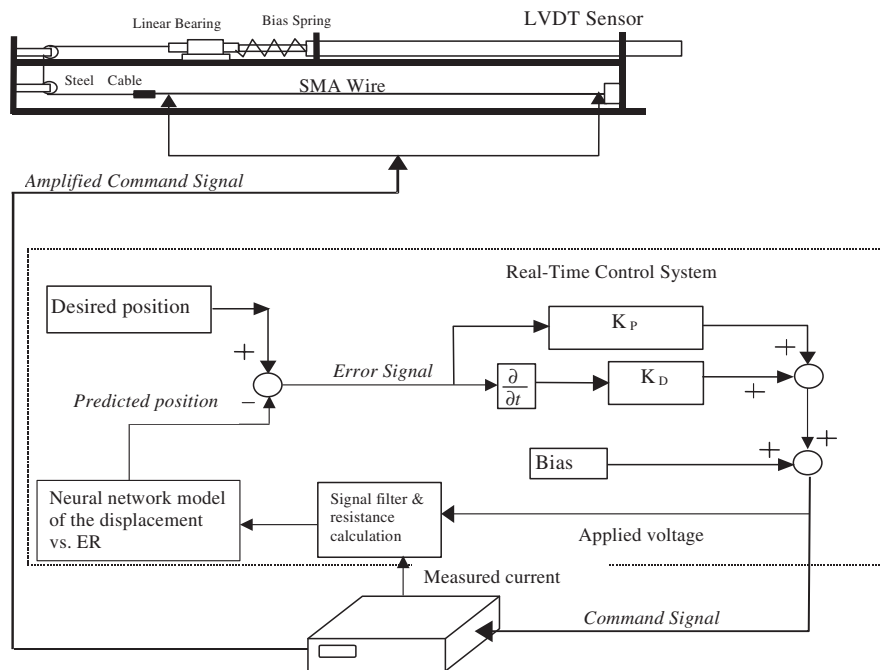


Figure 14. The block diagram of the ER feedback control system.

that the slider remained at the desired position for each step input. Figure 9(a) shows that the steady state error was less than 0.002 mm for each step input. Figure 9(b) shows the relationship between the ER and strain, with each curve having similar characteristics. This same trend was also observed for the major loops, as shown in figures 4, 6, and 8.

4. Modeling ER hysteresis using neural networks and position control design

As shown by the results in the previous section, the ER–strain relationship is hysteretic and is not fully repeatable. This relationship is complex in the minor loops and results in approximately a 15% displacement variation in the stable major loops. Even with this variation, the position of the SMA wire can still be estimated from the measured ER. For modeling purposes, one major hysteresis loop, shown in figure 10, was selected to represent the ER hysteretic behavior in the stable state. Although the choice of this representative loop will induce some errors, for some SMA wire actuators, this error may be acceptable.

In order to model the relationship between the ER and displacement of the representative loop, a multilayered neural network was designed. The multilayered neural network has a three-layer structure, with the one hidden layer having eight neurons as shown in figure 11. The two inputs are the ER and a ‘tag’ signal. The ‘tag’ signal is used since the displacement–ER curve cannot be represented by a one-to-one relationship due to the hysteresis. Since one ER value corresponds to two or three displacement values, the ‘tag’ signal is used to distinguish the different segments of the representative loop based on the slope change. The representative loop is divided into three segments: AB, BC and CD. The AB segment has a negative slope that corresponds to the heating process. The BC segment has a negative slope that represents the resistance increase in

cooling. In the same cooling process, the CD segment has a positive slope.

The training of the neural network is illustrated in figure 12. Data from the representative loop are used to train the neural network until the output produced corresponds well to the real output. The simulation results of the trained neural network and the real displacement of the NiTi wire actuator for the representative loop are shown in figure 13. The results demonstrate that the neural network accurately approximates the displacement as a function of ER.

Utilizing the developed neural network, a closed-loop position control system for the NiTi wire actuator was designed and implemented. In the block diagram of the control system shown in figure 14, the ER is computed using the applied voltage and the measured current on the NiTi wire. The trained neural network model estimates the displacement of the NiTi wire from the given ER value. The difference between the desired and predicted positions produces an error signal that is input into the PD controller. The control signal generated by the PD controller is increased using a programmable power amplifier before being applied to the wire to drive the SMA actuator. The LVDT sensor is used to measure the position of the slider for verification purposes.

Experiments were conducted to verify the accuracy of the developed closed-loop position control system for the NiTi wire actuator. In these tests, a multi-step position signal is sent to the control system. Each segment of the position command lasts for 30 s and increases (or decreases) 1 mm from the previous value. The desired displacement ranges from 1 to 7 mm. Figure 15 shows the controlled position response from a typical experiment. The average position error is approximately 7% in the steady state. The results also indicate that the control accuracy while the NiTi wire is being heated is much greater than when the wire is being cooled. Although the position control accuracy of the ER feedback

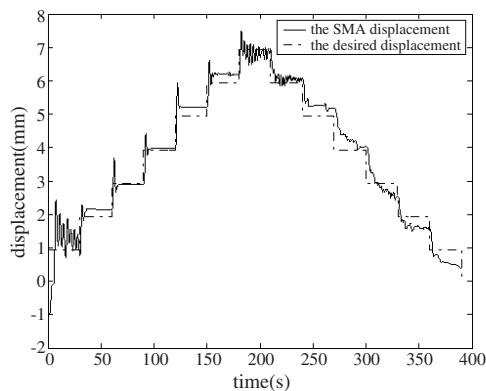


Figure 15. The displacement of the SMA actuator with only ER feedback control.

control is larger than that of the feedback control with a position sensor, the performance is still good and acceptable for many applications, especially considering that there is no position sensor used and there is an error induced by the choice of the representative major loop.

5. Conclusions

An electrical resistance (ER) feedback control system for position regulation of a spring-biased NiTi SMA wire actuator was developed. Experimental tests conducted on the SMA actuator demonstrated the existence of a hysteretic ER-strain relationship that depends on several activation conditions. A multilayered neural network model was implemented to simulate a representative major ER hysteresis loop and to predict the displacements using the ER values for feedback control purposes. A proportional-derivative (PD) position control system based on estimated displacement was designed and experimentally tested to illustrate that ER feedback control is a feasible alternative to position feedback control of SMA actuators for some applications.

Acknowledgments and disclaimer

The second author would like to acknowledge the support provided through an NSF CAREER grant (grant No 0093737) and a NASA cooperative agreement (No NCC3-839) in conducting

this research. Any opinions, findings, and conclusions or recommendations expressed in this material are those of the author(s) and do not necessarily reflect the views of the sponsors.

References

- [1] Tu K-Y, Lee T-T, Wang C-H and Chang C-A 1999 Design of a fuzzy walking pattern (FWP) for a shape memory alloy (SMA) biped robot *Robotica* **17** 373–82
- [2] Kudva J N, Sanders B, Pinkerton-Florance J and Garcia E 2001 Overview of the DARPA/AFRL/NASA smart wing phase 2 program *Smart Structures and Materials 2001: Industrial and Commercial Applications of Smart Structures Technologies (Newport Beach, CA, 2001)*; *Proc. SPIE* **4332** 383–9
- [3] Kuribayashi K 2000 Micro SMA actuator and motion control *Proc. 2000 Int. Symp. on Micromechatronics and Human Science (Nagoya, Japan, 2000)* (Piscataway, NJ: IEEE) pp 35–42
- [4] Brinson L C, Bekker A and Hwang S 1996 Deformation of shape memory alloys due to thermo-induced transformation *J. Intell. Mater. Syst. Struct.* **7** 97–107
- [5] Ikuta K, Tsukamoto M and Hirose S 1991 Mathematical model and experimental verification of shape memory alloy for designing micro actuator *Proc. IEEE Micro Electro Mechanical Systems* (Piscataway, NJ: IEEE) pp 103–8
- [6] Song G 2002 Robust position regulation of a shape memory alloy wire actuator *Proc. Inst. Mech. Eng. I* **216** 301–8
- [7] Troisfontaine N, Bidaud P and Dario P 1998 Control experiments on two SMA based micro-actuators *Experimental Robotics V (Lecture Notes in Control and Information Sciences vol 232)* (London: Springer) pp 490–9
- [8] Ikuta K, Tsukamoto M and Hirose S 1988 Shape memory alloy servo actuator system with electrical resistance feedback and application for active endoscope *Proc. 1988 IEEE Int. Conf. on Robotics and Automation vol 1*, (Piscataway, NJ: IEEE) pp 427–30
- [9] Pozzi M and Airoidi G 1999 The electrical transport properties of shape memory alloys *Mater. Sci. Eng. A* **273–275** 300–4
- [10] Raparelli T, Zobel P B and Durante F 2002 SMA wire position control with electrical resistance feedback *Proc. 3rd World Conf. on Structural Control (Como, Italy, 2002) vol 2*, (Chichester, England: John Wiley & Sons, Ltd) pp 391–8
- [11] Wu X D, Wu J S and Wang Z 1999 The variation of electrical resistance of near stoichiometric NiTi during thermo-mechanic procedures *Smart Mater. Struct.* **8** 574–8
- [12] Carballo M, Pu Z J and Wu K H 1995 Variation of electrical resistance and the elastic modulus of shape memory alloys under different loading and temperature conditions *J. Intell. Mater. Syst. Struct.* **6** 557–65